Supplementary information for

Optofluidic laser array based on stable high-Q Fabry-Pérot microcavities

Wenjie Wang,[a*] Chunhua Zhou,[a] Tingting Zhang,[a] Jingdong Chen,[a]
Shaoding Liu[a] and Xudong Fan[ab*]

[a]Key Lab of Advanced Transducers and Intelligent Control System of Ministry of Education,
Taiyuan University of Technology, 79 Yingze Street, Taiyuan 030024, P. R. China

[b]Department of Biomedical Engineering, University of Michigan,
1101 Beal Avenue, Ann Arbor, Michigan 48109, United States

[*]wangwenjie@tyut.edu.cn
[*]xsfan@umich.edu

I. Finesse measurement using the cavity scanning method

As an auxiliary method to characterize the p-c and p-p FP cavities in Type 1 and Type 2 chips, we measured the transmission spectrum at a fixed laser wavelength using the scanning cavity method.[1] Experimental setup is shown in Fig. S1. The wavelength of a single-mode cw laser was fixed at λ_0=561 nm. Plano mirror M1 (without any concave structure) was mounted in a one dimensional translation stage (Stage 1) that could move along the z direction and was controlled by a piezo actuator. Mirror M2 with an array of concave microwells on the surface was mounted on a translation stage (Stage 2) that provided four axes of adjustments, including the x and y direction and the two angular orientations. The cavity was first aligned with Stage 2 and then the cavity length was scanned along the z direction by the piezo actuator for a few free-spectral-ranges (FSRs) with the initial cavity length at 50 μm. The transmission spectrum was collected by a photo-detector that was connected to the oscilloscope. The finesse, F, can be obtained by F=FSR/δν, where δν is the FWHM (full-width at half-maximum) of the transmission peak using a Lorentzian fit. For a p-c FP cavity, the laser beam passed M1 and a concave microwell on M2. For the corresponding p-p FP cavity, the laser beam passed M1 and a place on M2 that did not have a microwell.

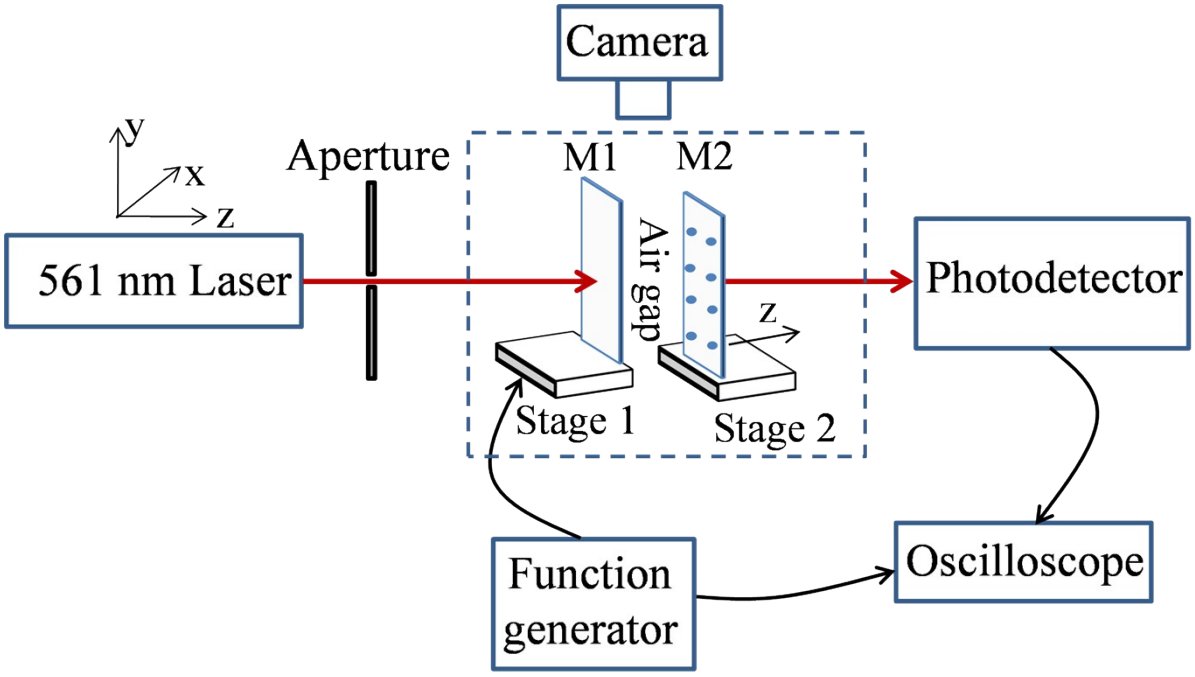

Figure S1 Experimental setup for finesse measurement using the scanning cavity method.

II. Q-factor and finesse estimation using the laser threshold

The lasing behavior of the cavity system for a given dye concentration can be described with a parameter γ(λ), the minimum fraction of the excited molecules,

$$\gamma(\lambda) = \frac{\sigma_a(\lambda_L)}{\sigma_a(\lambda_L) + \sigma_e(\lambda_L)}(1 + \frac{Q_{abs}}{Q_0}) \quad (1)$$

where σ_a and σ_e represent the absorption and emission cross section, respectively; $\lambda_L$is the emission wavelength; Q_0 is the empty cavity Q-factor when the cavity is filled with solvent in the absence of dye; Q_{abs} is the Q-factor related to the dye absorption, i.e.

$$Q_{abs} = \frac{2\pi n}{\lambda_L n_T \sigma_a(\lambda_L)} \quad (2)$$

where n and n_T denotes the refractive index of the solvent and the total concentration of dye molecules, respectively. According to the three-level model at steady state, γ is directly related to the pump threshold P_{th}. After a straightforward derivation, P_{th} is obtained as

$$P_{th} = \frac{8\pi h c^2 n^2 \Delta t}{\lambda_L^4 \lambda_p E(\lambda_L)} \times \frac{A(1+C)}{1 - BC} \quad (3)$$

where h, c, Δt, λ_P, and $E(\lambda_L)$ represent the plank constant, light velocity in vacuum, pulse width, pump wavelength, and fluorescence quantum distribution at emission wavelength, respectively; $A = \sigma_a(\lambda_L)/\sigma_a(\lambda_p)$, $B = \sigma_a(\lambda_L)/\sigma_e(\lambda_L)$, and $C = Q_{abs}/Q_0$.

The parameters and the Q-factor/finesses for the cavities in Fig. 3 are tabulated in Table S2.

III. Calculation of fluidic dome volume and cavity mode volume

1: Fluidic volume $V_d = \pi a^2 t$, where we use Gaussian fit $f = t \times exp(-\frac{x^2+y^2}{a^2})$ to approximate the surface profile of a concave microwell.

2: Optical cavity mode volume of TE_{00} mode

The electric field distribution $E(x,y,z)$ of standing waves in the resonator cavity is

$$E(x,y,z) \propto exp(-\frac{x^2+y^2}{w^2(z)})cos(\frac{2\pi}{\lambda}z) \quad (4)$$

where

$$w(z) = w_0 \times \left[1 + (\frac{\lambda z}{\pi w_0^2})^2\right]^{1/2} \quad (5)$$

with w_0 the minimum beam waist along z direction.

For the p-c FP microcavity, the radius of plano mirror is $R_1 = \infty$, and the radius of concave mirror is R_2 (we take R_2 as the minimum radius of surface curve of the concave microwell). Then we get $g_1 = 1 - t/R_1 = 1$, $g_2 = 1 - t/R_2$ and the beam waist for the plano and concave mirror is

$$w_1 = (\frac{t\lambda}{\pi})^{1/2}(\frac{g_2}{1-g_2})^{1/4}, \quad w_2 = (\frac{t\lambda}{\pi})^{1/2}(\frac{1}{g_2(1-g_2)})^{1/4} \tag{6}$$

The cavity length t is very short; and the calculated $w_1 \; and \; w_2$ are nearly the same (as shown in Table S3), simply we can get the optical cavity mode volume V_c of the p-c microcavity as

$$V_c = \iiint |E(x,y,z)|^2 \, dxdydz \approx \frac{1}{4}\pi w_1^2 t \approx \frac{1}{4}\pi w_2^2 t \tag{7}$$

The parameters, fluidic volume, and cavity mode volumes for the cavities in Fig. 5 are tabulated in Table S3.

Table S1: Summary of optofluidic lasers generated using different types of optical cavities

Cavity type	Pump conditions	Gain medium	Lasing (wavelength, threshold, Q_0 value)	Citations
FP cavity: Cr/Au mirrors, reflectivity 83% and 72%; optical cavity length 21.6 μm	Nd: YAG laser: 532 nm, 5 ns,10 Hz	R6G, 0.01 M	570 nm,30 mW/cm^2 (~30 μJ/mm^2)	Ref. [2]
Four-ring-cavity with total internal reflection	Nd: YAG laser: 532 nm, 0.5 ns, 5 kHz	R6G , 0.01 M	569 nm, 15 μJ/mm^2	Ref. [3]
FP cavity : Au coating on plano fiber end; cavity length 600 μm	Nd: YAG laser: 532 nm, 0.5 ns, 5 kHz	R6G , 0.01 M	25 μJ/mm^2	Ref. [4]
FP cavity: Au coating on plano fiber end, reflectivity 80%; cavity length 140 μm	Nd: YAG laser: 532 nm, 0.5 ns, 5 kHz	R6G, 1 mM	569 nm, 2 μJ/mm^2	Ref. [5]
FP cavity: Au coating on plano fiber end; cavity length 550 μm	Nd: YAG laser: 532 nm, 5 ns	R6G, 5 mM	569 nm	Ref. [6]
FP cavity: Au coating on plano fiber end; cavity length 18 μm	Nd: YAG laser: 532 nm, 0.5 ns	R6G, 1 mM	565 nm, 10 μJ/mm^2	Ref. [7]
FP cavity: two concave mirrors (curvatures, 10 mm and 50 mm), DBR coating, reflectivity>99.5%; cavity length 20 μm;	OPO: 465 nm, 5 ns, 10 Hz	eGFP, ~300 μM	850±200 pJ (focal lens 30 mm)	Ref. [8]
FP cavity: plano mirrors, DBR coating, reflectivity>99.5%; cavity length 18 μm;	OPO: 465 nm, 5 ns	GFP, 600±200 μM (in one bacterial cell)	160±10 nJ (focal lens 35 mm)	Ref. [9]
FP cavity: Plano mirrors, Ag coating, reflectivities >95% and > 80 % (λ>600 nm); cavity length ~125 μm	Nd:YAG laser: 355 nm, 5 ns, 10 Hz	DCM, 2 g/L in DMSO	~646 nm, ~110 nJ (4× microscope objective focal lens)	Ref. [10]
High-order (130th) Bragg grating	Nd: YAG laser: 532 nm, 0.5 ns, 5 kHz	R6G, 20 mM	582.7 nm, 20 μJ/mm^2	Ref. [11]
Phase shifted 15th order distributed feedback structure	Nd: YAG laser: 532 nm, 6 ns	R6G, 1 mM	567.3 nm, ~0.8 mJ/cm^2	Ref. [12]
15th-orderBragg grating	Nd: YAG laser: 532 nm, 6 ns	R6G, 2 mM	570 nm, 1 μJ	Ref. [13]
Third-order distributed Bragg grating	Nd:YAG laser: 532 nm, 5 ns, 10 Hz	R6G, 0.02M	581.41 nm, 65 μJ/mm^2(in ethanol); 582.72 nm, 40 μJ /mm^2 (in glycol); 587.86 nm, 10 μJ /mm^2 (in the mixture of ethanol and glycol)	Ref. [14]
Low-order (first, second, and third) distributed feedback resonators	Nd:YAG laser: 532 nm, 4.5 ns	R6G, 1 mg/mL (~2 mM)	569.1 nm, 78 nJ/pulse (~62 μJ/cm^2, 20 μm beam radius waist, 5× objective focal lens, second order grating)	Ref. [15]
Second order circular distributed feedback grating	Nd:YAG laser: 532 nm, 4.5 ns, 100 Hz	R6G, 1 mg/mL (~2 mM)	571.09 nm, 9.5 μJ/pulse (10× objective focal lens)	Ref. [16]
Droplet (levitated in air), diameter ~1mm	Nd:YAG laser: 532 nm, 5 ns, 10 Hz	R6G, 20 mM	~630 nm, ~500 mW	Ref. [17]
Ring resonator (out-diameter: ten to few hundreds of μm, wall thickness: a few μm)	OPO: 532 nm,10 ns, 20 Hz	R6G, 2 mM	600 nm, 25 nJ/mm^2 (estimated $\eta Q_0 \approx 4\times10^6$)	Ref. [18]
Droplets (diameters from 20 to	Nd:YAG laser:	R560 and R640	~590 and 675 nm,	

40 μm)	532 nm	5 mM	1 μJ/pulse (beam diameter 30 μm)	
Coupled optofluidic ring resonators	OPO: 532 nm,5 ns	R6G, 2 mM	570 nm, 6 μJ/mm^2	Ref. [20]
A ring shaped channel, inner, outer radius and depth 150, 170, and 40 μm	OPO: 532 nm, 5 ns, 20 Hz	R6G,1 mM	575 nm, ~15 μJ/mm^2 (estimated $Q_0 \approx 3.3\times10^4$)	Ref. [21]
Optofluidic ring resonators, inner diameter 70-90 μm, wall thickness 1-2 μm	OPO: 433 nm, 5 ns, 20 Hz	Quantum dots(QDs), 2 μM (in bulk solution)	660-665 nm, 0.1 μJ/mm^2 (estimated $\eta Q_0 \approx 1\times10^7$)	Ref. [22]
Photonic crystal slab, a square lattice of air cylindrical holes	Nd:YAG laser: 532 nm, 5 ns, 10 Hz	R6G, 1 mM	580 nm, 90 nJ/mm^2 (pump laser resonantly enhanced by a factor of 80) (derived $Q_0=8.3\times10^3$)	Ref. [23]
Biological tissues with scatters as the random resonator infiltrated with laser dye solution	Nd:YAG laser: 532 nm, 100 ps, 100 Hz	R6G	≤ 2 μJ/mm^2	Ref.[24]
Cortical bone from bovine femurs immersed in laser dye solution	OPO: 690 nm, 100 fs, 1 kHz	R800 in ethanol or (DMSO), weight ratio: 0.3%	15 mW, size of pump beam: 100 μm × 3 mm (estimated pump density: 50 μJ/mm^2)	Ref. [25]
Disordered optofluidic channel with structural disorder as the resonator	Nd:YAG laser: 532 nm, 6 ns, 20 Hz	R6G, 2.5 mM	80 μJ/mm^2	Ref. [26]
Disordered optofluidic channel with structural disorder as the resonator	Nd:YAG laser: 532 nm, 7 ns, 10 Hz	R6G, 2.5 mM	561.77 nm, 21 μJ/mm^2 (spectrum and intensity of laser can be selected by the pump profile)	Ref. [27]
Plano-concave FP cavity with DBR coating, cavity length = 31 μm	OPO: 532 nm, 5 ns, 20 Hz	R6G, 1 mM	599 nm, 90 nJ/mm^2 (derived $Q_0=5.6\times10^5$, F=4000)	Current work

Table S2: Parameters used for the calculation of Q_0-factor/Finesse in Section II

Dye concentration	1 mM			
Pump wavelength λ_p (nm)	532			
Absorption cross section at λ_p(cm^2)	1.9×10^{-16}			
Refractive index of the solvent n	1.366			
Quantum yield q	0.9			
Pulse width Δt (ns)	5			
Chips	**Type 1**		**Type 2**	
Microcavity	p-c cavity	p-p cavity	p-c cavity	p-p cavity
Lasing wavelengthλ_L (nm)	592	563	599	570
Absorption cross section at λ_L(cm^2)	1.4×10^{-19}	5.6×10^{-18}	5×10^{-20}	1.5×10^{-18}
Emission cross section at λ_L(cm^2)	1.1×10^{-16}	1.7×10^{-16}	1×10^{-16}	1.6×10^{-16}
Fluorescence distribution E(λ_L) (1/nm)	6.4×10^{-3}	1.2×10^{-2}	5.6×10^{-3}	1×10^{-2}
Q_{abs} at λ_L	1.7×10^{6}	4.5×10^{4}	4.8×10^{6}	1.6×10^{5}
A	7.5×10^{-4}	3.0×10^{-2}	2.6×10^{-4}	8.1×10^{-3}
B	1.3×10^{-3}	3.3×10^{-2}	4.8×10^{-4}	1×10^{-2}
$8\pi hc^2n^2\Delta t/\lambda_L^4\lambda_p E(\lambda_L)$ (μJ/mm^2)	33	22	36	24
P_{th} (μJ/mm^2)	0.33	8.55	0.09	1.1
Q_0	1.3×10^{5}	3.6×10^{3}	5.6×10^{5}	3.5×10^{4}
Cavity length L (μm)	49	46	31	22
Finesse ($=\lambda Q_0/2nL$)	575	16	4000	332

Table S3: Parameters used for the calculation of fluidic volume and cavity mode volume for Type 1 and Type 2 p-c cavities in Fig. 5.

p-c FP microcavity	**Type 1**	**Type 2**
Laser wavelength (nm)	590.6	600
Depth t (*i.e.*, cavity length) (μm)	4	8
a (μm)	24	70
Effective diameter d (μm)	34	100
Fluidic mode V_d(pL)	7	123
g_1	1	1
Radius R_2(μm)	78	306
g_2	0.9487	0.9739
Beam waist w_1(μm)	1.7983	3.0550
Beam waist w_2(μm)	1.8462	3.0957
Optical cavity mode V_c(fL)	11	60

References:

1. D. Hunger, T. Steinmetz, Y. Colombe, C. Deutsch, T. W. Hänsch, and J. Reichel, "A fiber Fabry–Perot cavity with high finesse," New J. Phys. **12**, 065038 (2010).
2. B. Helbo, A. Kristensen, and A. Menon, "A micro-cavity fluidic dye laser," J. Micromech. Microeng. **13**, 307–311 (2003).
3. J. C. Galas, J. Torres, M. Belotti, Q. Kou, and Y. Chen, "Microfluidic tunable dye laser with integrated mixer and ring resonator," Appl. Phys. Lett. **86**, 264101 (2005).
4. J. C. Galas, C. Peroz, Q. Kou, and Y. Chen, "Microfluidic dye laser intracavity absorption," Appl. Phys. Lett. **89**, 224101 (2006).
5. Q. Kou, I. Yesilyurt, and Y. Chen, "Collinear dual-color laser emission from a microfluidic dye laser," Appl. Phys. Lett. **88**, 091101 (2006).
6. G. Aubry, S. Méance, A.-M. Haghiri-Gosnet, and Q. Kou, "Flow rate based control of wavelength emission in a multicolor microfluidic dye laser," Microelectron. Eng. **87**, 765-768 (2010).
7. G. Aubry, Q. Kou, J. Soto-Velasco, C. Wang, S. Meance, J. J. He, and A. M. Haghiri-Gosnet, "A multicolor microfluidic droplet dye laser with single mode emission," Appl. Phys. Lett. **98**, 111111 (2011).
8. M. C. Gather, and S. H. Yun, "Single-cell biological lasers," Nature Photon. **5**, 406-410 (2011).
9. M. C. Gather, and S. H. Yun, "Lasing from Escherichia coli bacteria genetically programmed to express green fluorescent protein," Opt. Lett. **36**, 3299-3301 (2011).
10. A. J. C. Kuehne, M. C. Gather, I. A. Eydelnant, S.-H. Yun, D. A. Weitzad, and A. R. Wheeler, "A switchable digital microfluidic droplet dye-laser," Lab Chip **11**, 3716-3719 (2011).
11. S. Balslev, and A. Kristensen, "Microfluidic single-mode laser using high-order bragg grating and antiguiding segments," Opt. Express (2005).
12. Z. Li, Z. Zhang, T. Emery, A. Scherer, and D. Psaltis, "Single mode optofluidic distributed feedback dye laser," Opt. Express **14**, 696-701 (2006).
13. Z. Li, Z. Zhang, A. Scherer, and D. Psaltis, "Mechanically tunable optofluidic distributed feedback dye laser," Opt. Express **14**, 10494-10499 (2006).
14. M. Gersborg-Hansen, and A. Kristensen, "Optofluidic third order distributed feedback dye laser," Appl. Phys. Lett. **89**, 103518 (2006).
15. W. Song, A. E. Vasdekis, Z. Li, and D. Psaltis, "Low-order distributed feedback optofluidic dye laser with reduced threshold," Appl. Phys. Lett. **94**, 051117 (2009).
16. W. Song, A. E. Vasdekis, Z. Li, and D. Psaltis, "Optofluidic evanescent dye laser based on a distributed feedback circular grating," Appl. Phys. Lett. **94**, 161110 (2009).
17. H. Azzouz, L. Alkhafadiji, S. Balslev, J. Johansson, N. A. Mortensen, S. Nilsson, and A. Kristensen, "Levitated droplet dye laser," Opt. Express **14**, 4374-4379 (2006).
18. S. Lacey, I. M. White, Y. Sun, S. I. Shopova, J. M. Cupps, P. Zhang, and X. Fan, "Versatile opto-fluidic ring resonator lasers with ultra-low threshold," Opt. Express **15**, 15523-15530 (2007).
19. S. K. Tang, Z. Li, A. R. Abate, J. J. Agresti, D. A. Weitz, D. Psaltis, and G. M. Whitesides, "A multi-color fast-switching microfluidic droplet dye laser," Lab Chip **9**, 2767-2771 (2009).

20. W. Lee, H. Li, J. D. Suter, K. Reddy, Y. Sun, and X. Fan, "Tunable single mode lasing from an on-chip optofluidic ring resonator laser," Appl. Phys. Lett. **98**, 061103 (2011).
21. H. Chandrahalim, Q. Chen, A. A. Said, M. Dugan, and X. Fan, "Monolithic optofluidic ring resonator lasers created by femtosecond laser nanofabrication," Lab Chip **15**, 2335-2340 (2015).
22. A. Kiraz, Q. Chen, and X. Fan, "Optofluidic Lasers with Aqueous Quantum Dots," ACS Photonics **2**, 707-713 (2015).
23. B. Zhen, S.-L. Chua, J. Lee, A. W. Rodriguez, X. Liang, S. G. Johnson, J. D. Joannopoulos, M. Soljačić, and O. Shapira, "Enabling enhanced emission and low-threshold lasing of organic molecules using special Fano resonances of macroscopic photonic crystals," Proc. Natl. Acad. Sci. USA **110**, 13711-13716 (2013).
24. R. C. Polson, and Z. V. Vardeny, "Random lasing in human tissues," Appl. Phys. Lett. **85**, 1289-1291 (2004).
25. Q. Song, S. Xiao, Z. Xu, J. Liu, X. Sun, V. Drachev, V. M. Shalaev, O. Akkus, and Y. L. Kim, "Random lasing in bone tissue," Opt. Lett. **35**, 1425-1227 (2010).
26. B. N. Shivakiran Bhaktha, N. Bachelard, X. Noblin, and P. Sebbah, "Optofluidic random laser," Appl. Phys. Lett. **101**, 151101 (2012).
27. N. Bachelard, S. Gigan, X. Noblin, and P. Sebbah, "Adaptive pumping for spectral control of random lasers," Nature Phys. **10**, 426-431 (2014).